



Ab-initio calculations of the direct and hydrogen-assisted dissociation of CO on Fe(3 1 0)

Mohammad Reza Elahifard, Manuel Pérez Jigato*, J.W. (Hans) Niemantsverdriet

Schuit Institute of Catalysis, Eindhoven University of Technology, 5600 MB Eindhoven, The Netherlands

ARTICLE INFO

Article history:

Received 8 February 2012

In final form 6 March 2012

Available online 15 March 2012

ABSTRACT

Via the formation process of the adsorbed intermediates formyl (HCO) and hydroxy-carbene (COH), the thermodynamics of the hydrogen-assisted CO dissociation on Fe(3 1 0) is investigated by means of first-principles total-energy calculations. A comparison with direct CO dissociation in the presence of coadsorbed atomic hydrogen leads to the conclusion that the direct process is the only thermodynamically viable route for CO dissociation on Fe(3 1 0), with strongly endothermic formation energies for both intermediates, HCO and COH.

© 2012 Elsevier B.V. All rights reserved.

1. Introduction

The adsorption and dissociation of CO on metal surfaces has become representative in surface science as the workhorse for fundamental studies in industrial catalysis [1].

Within the last few years, giant strides have been taken in the theory of surface chemical reactivity, including the elucidation of the fundamental nature of CO activation on transition and noble metal surfaces, categorised as a late-transition state structure-sensitive reaction [2] that follows the universality principle [3]. Structure sensitivity makes reference to the role of active sites at surfaces (steps, kinks, edges and corners) on lowering reaction barriers whereas the concept of universality principle relies on establishing linear relations between activation barriers and product adsorption energies.

Not so successful is the general trend of semilocal exchange-correlation functionals of density-functional theory (DFT) of predicting the wrong adsorption site for CO on metal surfaces (the CO puzzle) [4–6]. Motivated by a too small HOMO–LUMO eigenvalue difference (and spin-triplet excitation energy) of the free CO molecule [7], as predicted by the theory, the problem manifests itself in the preference for high coordination adsorption sites for CO. Experimentally speaking, and at low coverages, both *fcc* and *hcp* metal surfaces tend to bind CO on the atop site in an upright configuration, whereas the semilocal functionals of DFT usually give the fourfold site on *fcc*(100) surfaces and the threefold site on *fcc*(111) and *hcp*(0001) surfaces as their most stable sites for CO adsorption [8–10]. It is important to note that a recent *ab initio* study [11] on several *bcc*(100) metal surfaces has found their high

reactivity towards CO dissociation to be correlated with the tilted geometry of adsorbed CO in the most stable configuration, as well as complying with the universality principle, and correctly predicting the fourfold hollow site, from DFT-RPBE, as the most stable site for CO adsorption at low coverages.

Both intrinsic metal reactivity and surface packing density are determining factors whereby either a direct or a hydrogen-assisted route is to govern CO dissociation in the presence of coadsorbed atomic hydrogen [12]. Driven by the formation of four intermediates (HCO, COH, HCOH and H₂CO), the hydrogen-assisted mechanism takes place on cobalt, iron and ruthenium surfaces [13–18]. In this work, only the energetics of formation for formyl and for hydroxy-carbene, in comparison to that for the direct dissociation of CO, are considered as thermodynamic indicators for the feasibility of the hydrogen-assisted path on Fe(3 1 0). On Co(0001), for example, the dissociation via HCO formation requires an overall activation barrier of 1.31 eV, while that for direct dissociation is much larger at 2.82 eV [14].

The adsorption of CO on the reactive iron surfaces is more exothermic and requires lower dissociation barriers (0.7–1.2 eV) than on cobalt [17,19], hence favouring the possibility of direct CO dissociation on iron surfaces in general. However, on the close-packed Fe(110) surface, the hydrogen-assisted CO dissociation barrier is substantially lower (1 eV difference) than the direct barrier [17], and this, in turn, is larger than the CO adsorption energy at saturation coverage. Therefore, Ojeda et al. [17] conclude that only the hydrogen-assisted dissociation mechanism is feasible on Fe(110). In contrast, on Fe(100), a more reactive surface than Fe(110), the overall barrier for the hydrogen-assisted route is higher than the direct barrier by 0.27 eV, along with an endothermic HCO formation step (+0.56 eV) [20]. The direct CO dissociation pathway provides the main reaction mechanism on Fe(100), although the

* Corresponding author. Fax: +31 402473481.

E-mail address: m.perezjigato@tue.nl (M. Pérez Jigato).

hydrogen-assisted route may compete under conditions where the molecule is surrounded by coadsorbed hydrogen atoms [20].

The spatial atomic arrangement of stepped and kinked surfaces may contain high index sites that contribute more than four atoms and provide suitable space for direct CO dissociation. Whereas on the flattest surfaces (maximum site index threefold or fourfold) the formation of HCO or COH could provide favourable pathways, there exist previous theoretical evidence [16,18] of a lower barrier for direct CO dissociation (as compared to the hydrogen-assisted route) on some stepped and kinked surfaces of Ru and Co. Here, we address the comparison of direct and hydrogen-assisted pathways on the stepped Fe(310) surface (its surface energy is in between those of Fe(100) and Fe(111) [19]), and compare it with the non-corrugated (100) and (110) surfaces [17,19,20].

2. Computational method

The thermodynamics for both mechanisms of CO dissociation on *bcc*-Fe(310), direct and hydrogen-assisted, is hereby investigated by means of *ab initio* calculations of CO + H coadsorbates, dissociation (C + O + H) and recombination products (CH + O, OH + C), and of the intermediates formyl (HCO) and hydroxycarbene (COH).

Within the formalism of spin-density-functional theory [21,22], total-energy calculations and geometry optimisations are carried out by means of the Projector-Augmented-Wave (PAW) method as implemented in the Vienna *ab-initio* SIMULATION Package (VASP, version 4.6.31) [23–26], with augmentation over planewaves, as opposed to augmentation over real-space grids [27].

The revised form of the Perdew, Burke and Ernzerhof (RPBE) [28–30] generalised-gradient approximation to the exchange-correlation energy functional and potential is employed for the self-consistent cycles, whereas the provided Fe, C, O and H PAW atomic potentials had been generated with a PBE atomic code. RPBE is known for its accuracy in predicting adsorption energies.

Iterative diagonalisations coupled to energy minimisations on the basis of the RMM-DIIS method lead to self-consistency in the Kohn–Sham equations, and fast-fourier transforms take the matrices from real to reciprocal space and viceversa. All calculations have been carried out on the $\begin{pmatrix} 2 & 2 \\ -1 & 1 \end{pmatrix}$ supercell. A cut-off energy of 400 eV for the planewave expansion of the single-particle wavefunctions, a first-order Methfessel–Paxton smearing polynomial with 0.1 eV width, and Monkhorst–Pack *k*-point sampling meshes of $7 \times 11 \times 1$ ($\begin{pmatrix} 2 & 2 \\ -1 & 1 \end{pmatrix}$) and $15 \times 15 \times 15$ (bulk) are employed [31] for the lattice sums. The Fe(310) surface is modelled by a five layer slab with 15 \AA° vacuum size. All layers are allowed to relax, under a force convergence criterion of 0.01 eV/ \AA° .

Since the low coverage regime is being investigated (and spurious finite size effects do appear) it is important to note that one CO molecule coadsorbed with one H atom in the two-dimensional $\begin{pmatrix} 2 & 2 \\ -1 & 1 \end{pmatrix}$ cell have each a $\frac{1}{4}$ ML local coverage. The resulting RPBE *bcc*-Fe equilibrium lattice constant is 2.855 \AA° , with a $\begin{pmatrix} 2 & 2 \\ -1 & 1 \end{pmatrix}$ lattice vector of 4.514 \AA° , and an ideal (310) interlayer distance of 0.90 \AA° , in agreement with previous results (2.87, 4.53 and 0.906) [32,33].

A transition-state search algorithm based on the climbing-image nudged elastic band approach (CI-NEB) [34] followed by transition-state structure refinement is applied to the computation of the reaction barrier.

3. Results and discussion

As a consequence of the small interlayer distance of the Fe(310) surface, both top and second layer atoms are actively involved in adsorption. On the other hand, a large number of active sites are available for adsorption on this stepped surface, which hints at the complexity of the envisaged coadsorption systems. Figure 1 shows the Fe(310) surface structure and Figure 2 contains the main results of this letter, in terms of geometries and relative adsorption energies for CO + H, C + O + H, CH + O, OH + C, HCO and COH, in their most stable configurations (except for the CO + H coadsorption system, for which both ground and first excited states are shown).

The three lowest energy configurations identified here for CO adsorption alone include two different tilted structures on the fourfold site (4f) with adsorption energies of 1.46 eV (α) and 1.13 eV (β), and a third tilted case with CO occupying the threefold site (3f) ($E_{\text{ads}} = 1.12$ eV). Both 4f occupying states correspond to the largest lengthening of the C–O bond, and they are expected to contribute to dissociation the most. The most stable adsorption configuration found here for CO is in agreement with previous reports by Sorescu [19] and Lo and Ziegler [35]. On the other hand, the most favourable sites for the separate H adsorption system correspond to 4f and 3f, the latter being more stable by 0.37 eV.

All possible combinations CO (α/β) + H (4f/3f) are considered for the coadsorption system, with any possible hydrogen site-switching being disregarded (Figure 2 shows the two lowest energy configurations). The most stable coadsorption state corresponds to the configuration (α)-CO + (3f₃)H, with $E_{\text{adsCO}} = 1.53$ eV. Whereas H adsorption on the 3f₃ site has a stabilising net effect on the CO adsorption energy (the general trend of H coadsorption on CO), which increases by 0.07 eV, the presence of H on the 4f₂ or on the 3f₁ sites, weakens the CO adsorption bond. Furthermore, the

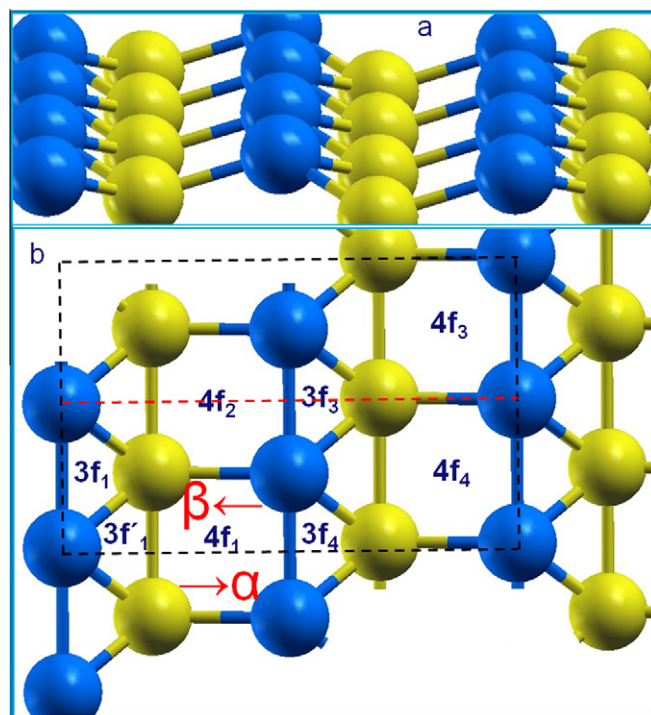


Figure 1. Structure of the two topmost layers of *bcc*-Fe(310): (a) slanted and (b) top view. The different threefold and fourfold hollow sites are depicted, and the $\begin{pmatrix} 2 & 2 \\ -1 & 1 \end{pmatrix}$ supercell is superimposed to the top view.

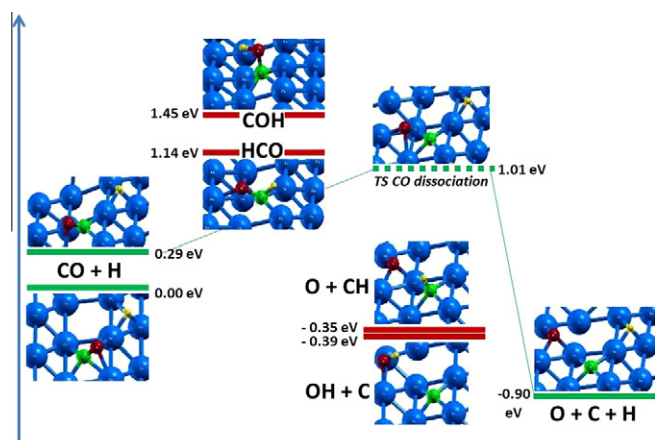


Figure 2. Common scale of relative adsorption energies that include the most stable HCO and COH adsorbate configurations on *bcc*-Fe(310), alongside the ground and first excited state for the CO + H ($3f_3$) coadsorption system, which correspond to CO in the α orientation (the configuration (α)-CO + ($3f_3$)H is the most stable coadsorption system and defines the zero reference energy) and in the β orientation, respectively (the configuration (β)-CO + ($3f_3$)H is the initial state to the CO-dissociation reaction leading to the most stable configuration of the dissociation products, C + O + H). Furthermore, the activation energy to dissociation of CO(β) + H($3f_3$) into the atomic adsorbates C + O + H and the thermodynamic state of the most stable configuration for the dissociation products C + O + H are shown. Finally, the thermodynamic state for the most stable recombination products HC + O and OH + C are depicted.

Table 1
C + O coadsorption energy.^a

H position	Without H ^a	4f ₂ ^b	4f ₃ ^b	3f ₁ ^b	3f ₃ ^b
C + O coadsorption energy (eV) C(4f ₁),O(3f ₁)	14.76	14.80	14.89	14.46	14.98
C + O coadsorption energy (eV) C(4f ₁),O(3f ₄)	14.31	14.45	14.35	14.17	14.31

^a Total binding energy per (C, O) atomic pair with respect to (a) clean surface and free atoms (C, O), and (b) H-pre-adsorbed surface and free atoms.

α -CO configuration is in general more stable than the corresponding β orientation by 0.3–0.35 eV.

Table 1 shows coadsorption energies for C + O both on the clean surface and on the hydrogen pre-adsorbed surface. The C + O coadsorption energy in the presence of hydrogen corresponds to the energy gain with respect to both free carbon and free oxygen atoms, after they are coadsorbed on the hydrogen pre-adsorbed surface (the probability of site-switching for H is disregarded). A comparison with the clean surface (no pre-adsorbed hydrogen present), shows that the effect of H, however slight, is larger for the coadsorbed C and O atoms than for adsorbed CO, implying a difference in the repulsive interaction H-(C + O) vs H-CO. A definite role of the C + O repulsion on the CO structural stability has been previously identified [36], and O + H is known to be more repulsive than C + H. In the atomically coadsorbed O + H system, both atoms occupy 3f sites on Fe(310), in contrast to the 4f sites they occupy on Fe(100) [20]. Therefore, the number of empty fourfold hollow sites active for CH formation after CO dissociation is much larger on Fe(310) than on Fe(100), which might suggest that Fe(310) is more resistant to poisoning.

Furthermore, the most stable configuration for the C + O + H coadsorption system (Figure 2), which, on the other hand results from CO dissociation within the CO(β) + H($3f_3$) coadsorption system, has a relative enthalpy of -0.90 eV, similar to the relative value on Fe(100) [20]. Since this C + O + H configuration has the lowest en-

thalpy of all possible adsorbed chemical species reported in this Letter (see Figure 2), the barrier to dissociation for the corresponding CO(β) + H($3f_3$) configuration is computed (transition state energy 1.01 eV; dissociation barrier 0.72 eV) and shown in Figure 2.

The lowest energy configuration for adsorbed formyl (relative adsorption energy 1.14 eV) corresponds to the CO fragment within HCO tilted towards the beta orientation (very similar to the CO structure in the CO + H coadsorption configuration for the first excited state, at 0.29 eV), with the H atom bonded to both the C atom and the metal surface (see Figure 2). On the other hand, the most stable adsorbed hydroxy-carbene (COH) configuration has a higher relative adsorption energy (1.45 eV), with its CO fragment being alpha-oriented and close to the surface normal, and carbon being the only atom bound to the metal surface and hydrogen being bound to oxygen, both forming a flat-tilted OH fragment within the COH adsorbate (see Figure 2).

The reaction energy of formation for both formyl and hydroxy-carbene is higher than the direct CO dissociation barrier (0.72 eV), which is sufficient evidence for concluding the thermodynamic non viability of the hydrogen-assisted CO dissociation mechanism on Fe(310). The dissociation barrier corresponds to a minimum-energy path that starts on the first-excited state of the CO + H coadsorption system (that with β -CO, at 0.29 eV), instead of starting on the lowest energy configuration (the CO + H coadsorbate with α -CO, at 0.0 eV). It corresponds to a situation that requires a thermal pre-excitation step of 0.29 eV for the CO + H ground state (α -CO) via the reorientation of the CO fragment from α to β . Since the unfavourable character of the hydrogen-assisted CO dissociation mechanism on Fe(310) is apparent, no further dissociation of neither HCO nor COH is to be investigated here.

Relative adsorption energies and geometries for the lowest energy configurations of both CH (coadsorbed with atomic O) and OH (coadsorbed with atomic C) formation processes, which take place after the direct CO dissociation in the presence of coadsorbed hydrogen, via different recombinations of the coadsorbed C + O + H system, are reported in Figure 2. The most stable structure for OH within OH + C corresponds to a lying-down-tilted geometry on the bridge site. Regarding the coadsorption CH + O system, the most stable configuration of the CH fragment is slightly tilted with respect to the normal, and occupying the 4f site. The OH + C formation process is slightly more exothermic than that for CH + O, and both are thermodynamically less favourable than the direct CO dissociation for the coadsorption system CO + H. The products of the recombination processes (HC + O and HO + C) are both thermodynamically more stable than the lowest energy configuration for the investigated intermediates of the hydrogen-assisted CO dissociation mechanism, viz adsorbed formyl (HCO) and adsorbed hydroxy-carbene (COH). A comparison of the recombination thermodynamics on Fe(310) with that on Fe(100) [20] is in order (see Fig. 3 in [20]). The lowest energy configuration for the HC + O coadsorption system on Fe(100) is the actual recombination product and has a relative adsorption enthalpy of -1.0 eV (defined with respect to the lowest energy configuration for coadsorbed CO + H), hence this is an exothermic reaction (initial state C + H + O, -0.93 eV), with a much more stable HC + O final state on Fe(100) than the equivalent on Fe(310), at -0.35 eV. On the other hand, the OH + C recombination product on Fe(100) (-0.31 eV relative energy for the lowest energy configuration) is similar in relative energy to that for Fe(310), at -0.39 eV. The OH + C lowest energy configuration on Fe(100) requires further rearrangement after the recombination reaction (final state energy -0.20 eV), which implies the OH group (upright configuration) that occupies the hollow site furthest to the C atom after the reaction, to migrate to the adjacent bridge site and to tilt away. No minimum energy path has been investigated for recombinations in the Fe(310) case.

4. Conclusion

In summary, the sequence followed by the adsorption energies of all the investigated species in their most stable configuration is $C + O + H < OH + C < CH + O < CO + H < HCO < COH$. The lowest energy state corresponds to the full dissociation product $C + O + H$, and the highest energy state to COH . Both COH and HCO are strongly endothermic with respect to the most stable $CO + H$ coadsorption system. In contrast, the fully dissociated $C + O + H$ coadsorption system as well as the two recombination products $CH + O$ and $OH + C$ are exothermic with respect to the lowest energy configuration of the $CO + H$ coadsorption system. Since the direct CO dissociation is an exothermic process (-0.90 eV reaction energy) and the formation energies for both COH and HCO are strongly endothermic, along with the fact that both formation energies are much higher than the direct dissociation barrier (0.72 eV), it can be concluded that the hydrogen-assisted CO dissociation route is thermodynamically unfavourable, and the direct path is the only feasible mechanism to CO dissociation on $Fe(310)$.

With the results of this and previous studies [17,19,20], we can now compare the direct and the hydrogen-assisted CO dissociation mechanisms on the close-packed (110), the flat but more reactive (100), and the stepped and even more reactive (310) surfaces of iron. On the close-packed $Fe(110)$ surface, the direct CO dissociation path has an activation energy of 1.95 eV [17]. In this case, weakening of the internal $C-O$ bond by pre-reaction with hydrogen is a feasible alternative, as the activation energy for HCO formation (0.92 eV) and subsequent splitting of the $C-O$ bond (0.78 eV) is only 1.70 eV [17]. On the flat but more open $Fe(100)$, the binding of the dissociation products C and O is stronger, making the dissociation more exothermic [20]. Late transition state reactions have been characterised by a direct correlation between exothermicity and low activation energies [1,12], in agreement with the Bronstedt–Evans–Polanyi relations [37,38]. Hence, for CO dissociation on iron surfaces, exothermicity drives the reaction.

On $Fe(100)$, the direct route is favoured and the dissociation path via HCO has a somewhat higher overall barrier. Nevertheless, direct CO dissociation needs a free empty site adjacent to the adsorbed CO molecule, and with sufficient coadsorbed hydrogen, the route via HCO might compete with direct dissociation, as the barriers differ only by 0.27 eV [20]. The stepped $Fe(310)$ surface exposes sites where the dissociation products C and O are even stronger bound than on the $Fe(100)$ surface. In fact, the hydrogen-assisted mechanism on $Fe(310)$ has reaction energies of formation for both adsorbed formyl and adsorbed hydroxy-carbene much higher than the value corresponding to the direct CO dissociation barrier (0.72 eV), hence, the activation energies accompanying the formation of both intermediates should be even higher than their reaction energy values of formation. On $Fe(310)$, the direct CO dissociation mechanism is therefore much more favoured than on $Fe(100)$. The interesting consequence is that on iron

particles that will expose both close-packed and more open facets, different activation routes for the dissociation of CO may coexist.

Acknowledgements

This work has been sponsored by the National Computing Facilities Foundation NCF (Grant SH-034-11) by granting access to the HUYGENS supercomputer at SARA with the financial support from the Netherlands Organisation for Scientific Research (Grant ECHO 700.59.041). The TU/e Chemical Engineering and Chemistry Department computer cluster has been used for calculations as well, and both Erik H Smeets and Ivo Filot are gratefully acknowledged for their support.

References

- [1] I. Chorkendorff, J.W. Niemantsverdriet, Concepts of Modern Catalysis and Kinetics, second Edn., Wiley-VCH Verlag, Weinheim, 2007.
- [2] R.A. van Santen, Acc. Chem. Res. 42 (2009) 57.
- [3] J.K. Norskov et al., J. Catal. 209 (2002) 275.
- [4] P.J. Feibelman et al., J. Phys. Chem. B 105 (2000) 4018.
- [5] P.H.T. Philipsen et al., Phys. Rev. B 56 (1997) 13556.
- [6] R.A. Olsen, P.H.T. Philipsen, E.J. Baerends, J. Chem. Phys. 119 (2003) 4522.
- [7] S.E. Mason, I. Grinberg, A.M. Rappe, Phys. Rev. B 69 (2004) 161401.
- [8] M. Gajdos, A. Eichler, J. Hafner, J. Phys.: Condens. Matter 16 (2004) 1141.
- [9] A. Stroppa, G. Kresse, New J. Phys. 10 (2008) 063020.
- [10] S. Pick, Surf. Sci. 601 (2007) 5571.
- [11] F.J.E. Scheijen, D. Curulla Ferre, J.W. Niemantsverdriet, J. Phys. Chem. C 113 (2009) 11041.
- [12] B. Hammer, J.K. Norskov, Adv. Catal. 45 (2000) 71.
- [13] G.A. Morgan Jr., D.C. Sorescu, T. Zubkov, J.T. Yates Jr., J. Phys. Chem. B 108 (2004) 3614.
- [14] O.R. Inderwildi, S.J. Jenkins, D.A. King, J. Phys. Chem. C 112 (2008) 1305.
- [15] M.P. Andersson et al., J. Catal. 255 (2008) 6.
- [16] S. Shetty, A.P.J. Jansen, R.A. van Santen, J. Am. Chem. Soc. 131 (2009) 12874.
- [17] M. Ojeda, R. Nabar, A.U. Nilekar, A. Ishikawa, M. Mavrikakis, E. Iglesia, J. Catal. 272 (2010) 287.
- [18] S. Shetty, R.A. van Santen, Phys. Chem. Chem. Phys. 12 (2010) 6330.
- [19] D.C. Sorescu, J. Phys. Chem. C 112 (2008) 10472.
- [20] M.R. Elahifard, M. Perez Jigato, J.W. Niemantsverdriet, ChemPhysChem 13 (2012) 89.
- [21] O. Gunnarsson, B.I. Lundqvist, Phys. Rev. B 13 (1976) 4274.
- [22] U. von Barth, L. Hedin, J. Phys. C: Solid State Phys. 5 (1972) 1629.
- [23] G. Kresse, J. Furthmüller, Comput. Mater. Sci. 6 (1996) 15.
- [24] G. Kresse, J. Hafner, Phys. Rev. B 49 (1994) 14251.
- [25] P.E. Blöchl, Phys. Rev. B 50 (1994) 17953.
- [26] G. Kresse, D. Joubert, Phys. Rev. B 59 (1999) 1758.
- [27] J. Enkovaara et al., J. Phys.: Condens. Matter 22 (2010) 253202.
- [28] J.P. Perdew, K. Burke, M. Ernzerhof, Phys. Rev. Lett. 77 (1996) 3865.
- [29] Y. Zhang, W. Yang, Phys. Rev. Lett. 80 (1998) 890.
- [30] B. Hammer, Phys. Rev. B 59 (1999) 7413.
- [31] H.J. Monkhorst, J.D. Pack, Phys. Rev. B 13 (1976) 5188.
- [32] J. Sokolov, F. Jona, P.M. Marcus, Phys. Rev. B 29 (1984) 5402.
- [33] W.T. Geng, M. Kim, A.J. Freeman, Phys. Rev. B 63 (2001) 245401.
- [34] G. Henkelman, B.P. Uberuaga, H. Jónsson, J. Chem. Phys. 113 (2000) 9901.
- [35] J.M.H. Lo, T. Ziegler, J. Phys. Chem. C 112 (2008) 3692.
- [36] T.C. Bromfield, D. Curulla-Ferré, J.W. Niemantsverdriet, ChemPhysChem 6 (2005) 254.
- [37] F.J. Abild-Pedersen et al., Phys. Rev. Lett. 99 (2007) 016105.
- [38] G. Jones et al., J. Phys.: Condens. Matter 2 (2008) 064239.